

VCKL-20564  
c.2

UNIVERSITY OF CALIFORNIA  
JUN 20 1971  
LIBRARY AND  
DOCUMENTS CENTER

# University of California

## Ernest O. Lawrence Radiation Laboratory

RAMAN SCATTERING FROM NEMATIC LIQUID-CRYSTALLINE AROMATICS

Habil M. Amer and Y.P. Shen

April 1971

**TWO-WEEK LOAN COPY**

*This is a Library Circulating Copy  
which may be borrowed for two weeks.  
For a personal retention copy, call  
Tech. Info. Division, Ext. 5545*

Berkeley, California

VCKL-20564  
c.2

## **DISCLAIMER**

This document was prepared as an account of work sponsored by the United States Government. While this document is believed to contain correct information, neither the United States Government nor any agency thereof, nor the Regents of the University of California, nor any of their employees, makes any warranty, express or implied, or assumes any legal responsibility for the accuracy, completeness, or usefulness of any information, apparatus, product, or process disclosed, or represents that its use would not infringe privately owned rights. Reference herein to any specific commercial product, process, or service by its trade name, trademark, manufacturer, or otherwise, does not necessarily constitute or imply its endorsement, recommendation, or favoring by the United States Government or any agency thereof, or the Regents of the University of California. The views and opinions of authors expressed herein do not necessarily state or reflect those of the United States Government or any agency thereof or the Regents of the University of California.

Submitted to the Journal of Chemical Physics

UCRL-20564  
Preprint

UNIVERSITY OF CALIFORNIA

Lawrence Radiation Laboratory  
Berkeley, California

AEC Contract No. W-7405-eng-48

RAMAN SCATTERING FROM NEMATIC LIQUID-CRYSTALLINE AZOXYBENZENES

Nabil M. Amer and Y. R. Shen

April 1971

34

Raman Scattering from Nematic Liquid-Crystalline Azoxybenzenes

Nabil M. Amer and Y. R. Shen

Department of Physics, University of California  
and

Inorganic Materials Research Division,  
Lawrence Radiation Laboratory  
Berkeley, California 94720

ABSTRACT

We have investigated the Raman spectra of four nematic members of the homologous series 4,4'-bis (alkoxy) azoxybenzene in the solid, nematic, and liquid phases for a spectral range of 10 - 1900  $\text{cm}^{-1}$ . These spectra show great similarity, as one would expect from the similarity of their molecular structure. A few Raman modes, particularly the intermolecular ones, exhibit quasi-discontinuous changes at the phase transitions. These changes are qualitatively interpreted as the result of modification of the intermolecular interaction induced by the phase transitions.

## I. INTRODUCTION

In the early days, Raman spectroscopy was mainly restricted to the investigation of molecular vibrations of individual molecules. With the invention of the laser, modern Raman spectroscopy has acquired considerable improvement both in resolution and sensitivity. It is now possible to investigate easily the effect of intermolecular interaction on the vibrational spectra and to follow the change of spectrum during phase transition.<sup>1</sup> In a previous paper<sup>2</sup> we have used Raman scattering to probe the phase transitions of the nematic compound p-azoxydianisole (PAA). In order to gain a better understanding of the interaction between the molecules of this type of nematic compounds in their different phases, and to help in the assignment of the observed Raman modes, we have extended our study to other nematic members of the homologous series of 4,4'-bis (alkoxy) azoxybenzene. In this paper, we report our Raman results on the four nematic compounds: p-azoxydianisole (PAA), p-azoxydiphenotole (PA $\Phi$ ), 4,4'-bis (pentyloxy) azoxybenzene (PAB), and 4,4'-bis (hexyloxy) azoxybenzene (HAB). These compounds have the chemical structure  $\text{RO}-(\text{C}_6\text{H}_4)-\text{N}_2\text{O}-(\text{C}_6\text{H}_4)-\text{OR}$ , where R is the alkyl chain of different lengths for different compounds as shown in Table I. In the liquid phase, where the molecules rotate and translate rather freely, one expects the Raman spectra of the four compounds to be quite similar except for the modes associated with the alkyl chain. On the other hand, in the nematic and solid phases, the spectra should reflect the effects of intermolecular interaction due to ordering of the molecules.

In Section II, we give a brief description of the experimental procedure and apparatus. In Section III, the Raman spectra of the four compounds in the three phases are presented. Phase transitions are monitored by the quasi-discontinuous change in the spectra. The results are interpreted using the known molecular structure of these compounds in different phases. Finally, in Section IV, the results are summarized and a few general comments are made.

## II. EXPERIMENTAL TECHNIQUES

The experimental setup<sup>3</sup> consisted of a Spectra-Physics Model 125 He-Ne laser, operated at 6328 Å, serving as the exciting source. Light, scattered in a direction normal to the direction of the exciting beam, was collected and analyzed by a Spex Model 1400 double monochromator. The slit widths were 2,3,2  $\text{cm}^{-1}$  respectively. Detection was accomplished via a cooled photomultiplier operated in conjunction with photon counting equipment. The spectrum was then stored and displayed on a multichannel analyzer.

To insure close temperature control of the sample, a Cu block immersed in an oil bath was used. The bath was a double walled glass dewar fitted with the appropriate optical windows. Temperature control was performed with a Hallikainen Thermotrol unit, and the sample temperature was monitored with a calibrated thermistor and recorded continuously. For a given run of two hours, fluctuations were less than 0.035°C.

The four compounds investigated were obtained from Eastman Organic Chemicals and were recrystallized three times to insure a higher degree

of purity. All solid samples were investigated in the polycrystalline form.

The vibrational frequencies were determined using the emission lines of a neon lamp as an absolute source for frequency calibration. In all four compounds, there is a Raman mode at  $1095 \text{ cm}^{-1}$ . This mode shows no appreciable change ( $\leq 15\%$ ) in its integrated intensity as the compounds change phases; therefore, it was used as the internal calibration line for our intensity measurements. The intensities reported below have an accuracy well within  $\pm 20\%$ .

Elastic scattering of light tends to deteriorate the quality of the spectrum near the laser line. In order to minimize the noise background from such scattering, we made use of the iodine filter technique<sup>4</sup> in recording the Raman spectrum between 0 and  $100 \text{ cm}^{-1}$ . The  $5145 \text{ \AA}$  line from an  $\text{Ar}^+$  laser of Coherent Radiation Model 52, operated in single mode was used as the exciting light source. A glass cell 15 cm long, filled with iodine vapor and maintained at  $95^\circ\text{C}$  was inserted between the sample and the entrance slit of the double monochromator. The sharp and strong absorption of  $\text{I}_2$  at  $5145 \text{ \AA}$  enabled us to obtain Raman spectra, even of the polycrystalline solids, to within  $10 \text{ cm}^{-1}$  of the laser line without any appreciable background.

### III. RESULTS AND DISCUSSION

For each compound, a spectral range of  $\pm 1900 \text{ cm}^{-1}$ , about the exciting frequency, was investigated in the solid, nematic, and liquid phases. Figs. 1-4 are traces of the complete Raman spectra, on the Stokes side, of these compounds. They are characterized by the

existence of several intense and sharp modes (of the same order as the  $992\text{ cm}^{-1}$  line of pure benzene). In addition, each spectrum has a number of broad and weaker bands. As the compounds change from solid to nematic and then to the liquid phase, a few modes disappear while most of them decrease in intensity and become broader. Generally, very little difference is observed between the spectra of the nematic and isotropic states, with the exception of the persistence of two modes at  $40$  and  $52\text{ cm}^{-1}$  in the nematic phase of PAA; they both disappear in the isotropic liquid. This indicates that the effect of intermolecular interaction on internal vibrational modes is weak, and/or the ordering in the molecular structure of the nematic phase does not change appreciably the intermolecular interaction. The low-frequency modes which disappear in the liquid phase are presumably the intermolecular modes or the lattice modes. They provide a measure of the strength of intermolecular interaction in the substance.

The spectra of the isotropic phase of the four compounds, PAA, PA $\phi$ , PAB, and HAB, should reflect the effects of the alkyl chain on the vibrational modes of the individual molecules. As shown in Figs. 1a - 4a, the spectra of the four compounds are very similar. Small differences, mainly in the form of changes in the relative intensities and small frequency shifts of the corresponding modes, are evident. Some weak modes which appear in one compound may be too weak to be detectable in the others, but all the stronger ones, except the one near  $1140\text{ cm}^{-1}$ , do have a one-to-one correspondence in all the compounds. These results indicate that the coupling between the end

groups and the rest of the molecule is rather weak, so that the addition of methylene groups to both ends of the molecule does not affect the vibrational spectrum of the molecule appreciably.

In the solid phase (Figs. 1C - 4C), the spectral lines are considerably sharper as a result of the molecules losing their rotational and translational freedom. More detailed structure of the spectra can now be seen and the effect of intermolecular interaction on certain vibrational modes is readily detectable. The spectral data are summarized in Table II, where we list the Raman frequencies of the four compounds in the solid state. The integrated intensity of various lines is given in arbitrary units normalized against the  $1095 \text{ cm}^{-1}$  mode. We have also listed the IR data and assignments of Maier and Englert.<sup>5-7</sup> It is interesting to note that most of the IR modes have their counterpart in the Raman spectra. This is not unexpected since these molecules possess low symmetry. We have also reproduced the Raman data of Freymann and Servant<sup>8</sup> and Zhdanova et al.<sup>9</sup> for PAA. Thanks to the recently developed techniques for Raman spectroscopy<sup>1,3</sup> our spectra are of much better quality than those reported previously.<sup>8,9</sup> To our knowledge, no Raman study of PA $\phi$ , PAB, and HAB has ever been reported.

The spectral range shown in Figs. 1-4, can be divided into five regions of interest:  $0 - 100 \text{ cm}^{-1}$ ,  $100 - 1100 \text{ cm}^{-1}$ ,  $1100 - 1225 \text{ cm}^{-1}$ ,  $1225 - 1300 \text{ cm}^{-1}$ , and  $1300 - 1625 \text{ cm}^{-1}$ . This division is based on the response of these spectral regions to the change in phase and to the change in the composition of the end groups. No Raman line appears

between  $1625\text{ cm}^{-1}$  and  $1900\text{ cm}^{-1}$ .

For the spectral region between  $1300$  and  $1625\text{ cm}^{-1}$ , the spectra of all the four compounds show no change with temperature in going from liquid to nematic and then to solid, except for a narrowing of the lines. There is also a close similarity in the spectra of the four compounds. The relative intensities of several modes do change from one compound to the next, but the frequency shifts of the corresponding modes are very small. These modes clearly do not belong to the methylene group in the alkyl chain. Their assignment, as suggested by Maier and Englert<sup>6</sup> is given in Table II.

The spectral region from  $1225$  to  $1300\text{ cm}^{-1}$  shows a rather drastic change as the substances change from the solid to the nematic phase. No further change is observed in the nematic-to-liquid phase transition. While the solid spectra of the four compounds in this region are fairly different, their nematic and isotropic spectra are still quite similar. They are characterized by two broad bands with the weaker one at lower frequency. In PAA, PAB, and HAB, the strong band is at  $1275\text{ cm}^{-1}$  and the weak one at  $1246\text{ cm}^{-1}$ , and in PA $\Phi$ , the former shifts to  $1270\text{ cm}^{-1}$ . The detailed spectra in this region for the four compounds in the three phases are reproduced in Figs. 5-8. For solid PAA, the composite spectrum can be decomposed into four modes at  $1246$ ,  $1252$ ,  $1261$ , and  $1276\text{ cm}^{-1}$  with the relative intensities being 4:1:4:6. As we reported earlier,<sup>2</sup> the three modes at lower frequencies decrease quasicontinuously at the solid-to-nematic phase transition. All the lines broaden and finally merge into two broad bands.<sup>10</sup>

However, the integrated intensity of the  $1276 \text{ cm}^{-1}$  line does not seem to change, but the linewidth increases quasidiscontinuously at the transition. The above description also applies to the spectra of the other compounds in this region. The weaker one of the two broad bands in the nematic phase increases in intensity at the nematic-to-solid transition. The stronger one gets sharpened, distorted, or even split in going to the solid phase, but its integrated intensity remains essentially unchanged.

The above results indicate that the modes in this spectral region are strongly influenced by intermolecular interaction. The qualitative feature can be understood from the molecular structure of the compounds in different phases. The crystal structure of PAA and PA $\Phi$  has been studied by Bernal and Crawfoot<sup>11</sup> and more recently by Krigbaum et al.<sup>12</sup> The molecules  $\text{RO}-(\text{C}_6\text{H}_4) - \text{N}_2\text{O} - (\text{C}_6\text{H}_4) - \text{RO}$  are fixed in regular positions with the long axes aligned approximately perpendicular to the (100) plane. They form an imbricated structure with the benzene rings of the two neighboring molecules either facing,<sup>11</sup> or perpendicular to,<sup>12</sup> each other. The RO groups should then be in close contact with the  $\text{N}_2\text{O}$  groups. There are altogether four molecules in each unit cell. We expect that the same structure also describes the crystalline phase of PAB and HAB. In the nematic phase, the molecules are no longer rigidly fixed in position. They are still well aligned, but they can rotate more or less freely about their own long axes.<sup>13</sup> Because of the permanent dipole attached to the RO group, we expect that the end groups of a given molecule interact more strongly with neighboring molecules.

and therefore cannot rotate as freely as the rest of the molecule. In the liquid phase, all long-range ordering breaks down, including ordering in the molecular alignment.

According to Maier and Englert,<sup>5,6</sup> the modes between 1225 and 1300  $\text{cm}^{-1}$  should correspond to the internal vibrational modes ( $\omega_3$  and  $\omega_4$ ) of the phenyl ring. From the crystal structure of the nematic compounds, we realize that these modes are likely to be affected by intermolecular interaction between the highly polarizable phenyl rings of the neighboring molecules. Such interaction decreases sharply in transition to the nematic phase as the molecules acquire freedom to translate and to rotate. As a result, the intensities of those modes which are affected by the interaction may change suddenly as we have observed. Furthermore, the onset of the rotational freedom in the phase transition gives rise to the sudden broadening of all the modes.

The spectral region between 1100 - 1225  $\text{cm}^{-1}$  also shows pronounced change in some of the modes during the solid-nematic phase transition. In particular, the mode around 1141  $\text{cm}^{-1}$  shows significant changes. It grows from virtual non-existence in PAA into a weak line in PA $\Phi$  and PAB, and finally, into a strong line in HAB. This mode should therefore belong to the end groups of the molecules, and is probably the twisting mode  $\tau(\text{CH}_2)$  of the alkyl chain, as suggested by Maier and Englert.<sup>6</sup> Then, we would expect from the crystal structure of these compounds that this mode also should be susceptible to change of phases through the intermolecular interaction between RO and NON groups of neighboring molecules. This is indeed the case and is most clearly observed in HAB.

As HAB changes from solid to nematic, the integrated intensity of the mode decreases by about 50%, and the line broadens. Little change is observed as the compound becomes isotropic liquid. In Fig. 9, we present the line intensity as a function of temperature. Emphasis is around the phase transitions. We notice that the curve exhibits a characteristic quasi-discontinuity at the solid-nematic transition.

Another mode of interest in this region appears at  $1171\text{ cm}^{-1}$  in the nematic and liquid phases of all four compounds. This mode is fairly strong and has been assigned as the  $\gamma(\text{CH}_3)$  mode of the alkyl chain.<sup>6</sup> When the compounds undergo transition to the solid phase, this mode remains unshifted in frequency in PAA; but in PA $\Phi$  and PAB, it shifts quasi-discontinuously to  $1178\text{ cm}^{-1}$ , and in HAB, to  $1176\text{ cm}^{-1}$ . The integrated line intensity however remains the same in the transition. In Fig. 10, we show, as an example, the temperature dependence of the shift for the mode in PA $\Phi$ . The strong intermolecular interaction between RO and NON of neighboring molecules in the solid phase is clearly responsible for the observed shift. However, it is somewhat surprising that the same mode does not show observable shift in PAA. Intuitively, we would expect the intermolecular interaction to loosen the internal mode and therefore decrease its vibrational frequency, as is usually the case. However, this may not be true in general and our results here show just the opposite.

The  $1188\text{ cm}^{-1}$  mode of HAB in the nematic or liquid phase also shifts to  $1192\text{ cm}^{-1}$  in transition to the solid phase. The corresponding mode at  $1186\text{ cm}^{-1}$  in PAA and at  $1188\text{ cm}^{-1}$  in PAB remains, however,

unshifted, and in  $PA\Phi$ , it is below our signal level.

The modes in the spectral region between 100 and 1100  $\text{cm}^{-1}$  show no observable change in either line intensities or frequencies as a function of temperature or phase, although they do get rotational broadening in the solid-to-nematic transition. All these modes are relatively weak, except the ones at 911  $\text{cm}^{-1}$  and 1095  $\text{cm}^{-1}$ . Some of them do not show up in the higher members of the homologous series presumably because they are below our detection level. Maier and Englert<sup>6</sup> have assigned the modes above 650  $\text{cm}^{-1}$  in this region (Table II), but the available tables on molecular vibrations<sup>14</sup> show that no mode attached to any molecular group in the nematic molecules would have a frequency lower than 650  $\text{cm}^{-1}$ . We believe that the modes below 600  $\text{cm}^{-1}$  are probably combination modes since their frequencies agree to within a few  $\text{cm}^{-1}$  with the difference frequencies of the observed strong lines in the region of 900 - 1600  $\text{cm}^{-1}$ . The weak modes between 600  $\text{cm}^{-1}$  and 900  $\text{cm}^{-1}$  can also be the combination modes arising from the anharmonic interaction of modes at higher frequencies, which we have not investigated.

Finally, the spectral region between 0 and 100  $\text{cm}^{-1}$  is of great interest. In solid PAA, we previously reported the observation of three Raman modes at 40, 52, and 72  $\text{cm}^{-1}$ .<sup>2</sup> With the  $I_2$  filter techniques,<sup>4</sup> we were able to detect an additional sharp mode at 21  $\text{cm}^{-1}$ . All the four modes remain unchanged both in frequency and in intensity as the temperature increases from 20°C up to 114°C (about 2.5°C below the solid-nematic transition temperature). In undergoing transition from

solid to nematic, the intensities of these modes change quasi-discontinuously, but their frequencies remain unshifted within our resolution limit ( $< 2 \text{ cm}^{-1}$ ). The  $21 \text{ cm}^{-1}$  and  $72 \text{ cm}^{-1}$  modes disappear in the nematic phase, but the  $40 \text{ cm}^{-1}$  and the  $52 \text{ cm}^{-1}$  modes persist. Then, the latter two modes also disappear quasi-discontinuously at the nematic-to-liquid transition. From these results, we conclude that these low-frequency modes are most likely the intermolecular modes between the  $\text{CH}_3\text{O}-(\text{C}_6\text{H}_4)-\text{N}_2\text{O}$  groups of neighboring molecules, and should be affected primarily by short-range ordering.<sup>2</sup> Recently, Bulkin and Prochaska<sup>15</sup> have reported the Raman spectra of a PAA single crystal in the same spectral region. The spectrum is better resolved and clearly indicates the presence of a few other modes. Their spectrum of polycrystalline PAA also shows only four modes, but their results of spectral change as a function of temperature is different from ours. Consequently, their interpretation of the low-frequency modes is also different from ours. In particular, we see no evidence of the existence of soft modes shifting towards zero frequency in approaching the solid-nematic transition. We believe that near phase transitions, temperature stability of the sample is of prime importance for obtaining reproducible spectra. That we can control our sample temperature to within  $\pm 0.03^\circ\text{C}$  makes us confident in our results.

In solid PA $\Phi$  and PAB, we have observed one broad band at  $54 \text{ cm}^{-1}$  and at  $37 \text{ cm}^{-1}$  respectively. This low-frequency mode disappears quasi-discontinuously, without detectable frequency shift at the solid-to-nematic transition. In HAB, no low-frequency mode was detected.

These results are consistent with the assertion that the low-frequency modes are the intermolecular modes connected with the end groups. A longer alkyl chain in the end group means a larger molecular weight for the end group, and hence a smaller frequency for the intermolecular vibrational mode.

In analyzing our data, we have also sought to verify the recent suggestion by Callender and Pershan<sup>16</sup> that the rotational side bands of a sharp Raman mode may be observable for compounds in the nematic phase. Our results indicate a clear onset of rotational broadening of all sharp lines at the solid-to-nematic transition; however, no discrete rotational side bands were detected. This is, in fact, what one would expect from the usually strong lifetime broadening of vibrational modes in condensed matter.

#### IV. CONCLUSION

We have shown the similarity, in the Raman spectra, of the nematic members of the homologous series of 4,4'-bis (alkoxy) azoxybenzene. The results help us in making assignments of the observed lines to the various intra- and inter-molecular vibrational modes. We have also shown the effects of phase transitions on the Raman spectra. They can be qualitatively interpreted in terms of the change in the inter-molecular interaction from the known modes of molecular structure of the nematic compounds in different phases.

The spectral change shows the characteristic quasi-discontinuity at the phase transitions (see Figs. 9 and 10). In principle, it can be used to investigate the nature of the phase transitions. For a

quantitative interpretation, statistical calculations, based on some model of order-disorder phenomena,<sup>17</sup> should be carried out. Since the Raman spectra here are primarily affected by short-range ordering, a calculation taking into account only the nearest-neighbor interaction would probably be sufficient.

## REFERENCES

1. See, for example, Light Scattering Spectra of Solids, edited by G. B. Wright (Springer-Verlag, Inc., New York, 1969).
2. N. M. Amer, Y. R. Shen, and H. Rosen, Phys. Rev. Letters 24, 718 (1970).
3. For a complete description of the photon counting setup, see D. Landon and S. P. S. Porto, Appl. Opr. 4, 762 (1965).
4. For a brief description of this technique, see W. L. Peticolas, G. W. Hibler, J. L. Lippert, A. Peterlin, and H. Olf, Appl. Phys. Letters 18, 87 (1971).
5. W. Maier and G. Englert, Z. Elektrochem. 62, 1020 (1958).
6. W. Maier and G. Englert, Z. Physik. Chem. N.F. 19, 168 (1959).
7. Some limited infrared spectra of PAA and PA $\Phi$  have been published by B. Bulkin, D. Grumbaum, and A. Santoro, J. Chem. Phys. 51, 1602 (1969).
8. R. Freymann and R. Servant, Ann. Phys. 20, 131 (1945).
9. A. S. Zhdanova, L. F. Morozova, G. V. Peregudov, and M. M. Sushchinskii, Opt. Spektrosk. 26, 209 (1969) [Trans. Opt. Spectros. (USSR) 26, 112 (1969)].
10. Assuming that the vibrational modes are symmetric in nature, one can decompose the spectrum of solid PA $\Phi$  into additional modes occurring at 1253, 1262, and 1271  $\text{cm}^{-1}$ ; and that of HAB into another weak mode at 1261  $\text{cm}^{-1}$ .
11. J. D. Bernal and D. Crowfoot, Trans. Farad. Soc. 29, 1032 (1933).
12. W. R. Krigbaum, Y. Chatani, and P. G. Barber, Acta Cryst. B26, 97 (1970).

13. See, for example, A. Saupe, *Angew. Chem. International: edition* 7, 97 (1968).
14. M. Magat. *Tables Annuelles de Constants et Données Numeriques*, Vol. 12 (1937).
15. B. J. Bulkin and F. T. Prochaska, *J. Chem. Phys.* 54, 635 (1971).
16. R. Callender and P. S. Pershan, *Phys. Rev. Letters* 23, 947 (1969).
17. See, for example, H. A. Bethe, *Proc. Roy. Soc. (London)*, 150A, 552 (1935); F. C. Nix and W. Shockley, *Revs. Modern Phys.* 10, 1 (1938).

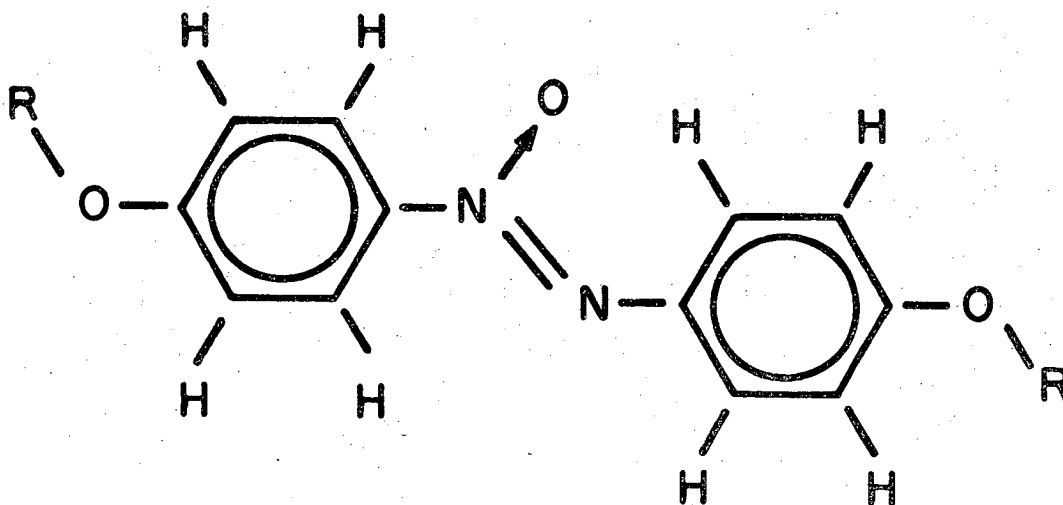
TABLE CAPTIONS

Table I. Chemical Structure, Abbreviations, and Nematic Temperature range for the Compounds Studied.

Table II. Frequencies<sup>+</sup>, Intensities, and Assignments of the Compounds Studied.

Table I

Chemical Structure, Abbreviations, and Nematic Temperature Range for the Compounds Studied



R	Name	Abbreviation	nematic range (°C)
CH <sub>3</sub>	4,4'-azoxydianisole	PAA	116-134
C <sub>2</sub> H <sub>5</sub>	4,4'-azoxydiphenotole	PAΦ	136-168
C <sub>5</sub> H <sub>11</sub>	4,4'-bis(pentyloxy)azoxybenzene	PAB	78-123
C <sub>6</sub> H <sub>13</sub>	4,4'-bis(hexyloxy)azoxybenzene	HAB	84-127

XBL 714-772

Table II. Frequencies, <sup>†</sup> Intensities, and Assignments of the Studied Compounds.

This work	PAA			PAΦ		PAB		HAB		Assignment (Ref. 6)
	Ref. 8	Ref. 9	Ref. 6	This work	Ref. 6	This work	Ref. 6	This work	Ref. 6	
21 (6)*						37 <sup>B</sup> (6)				
40 (7)										
52 (9)				54 <sup>B</sup> (14)						
72 (18)										
210 <sup>B</sup> (?)	213									
234 <sup>B</sup> (?)										
317 (5)	313			318 <sup>B</sup> (6)		317 <sup>B</sup> (7)				
360 <sup>B</sup> (?)	365									
417 (5)										
474 (7)				467 <sup>B</sup> (4)						
494 (5)						494 <sup>B</sup> (1?)				
536 (2)		543								
611 <sup>B</sup> (2?)		618								
629 <sup>B</sup> (3)		637		628 <sup>B</sup> (6)		628 <sup>B</sup> (7)		629 <sup>B</sup> (7)		
670 (6)		678	667		669	671 <sup>B</sup> (3)	665		663	Γ <sub>1</sub>
			717		718		718 <sup>sh</sup>		718	} Γ <sub>3</sub>
725 (5)		733	723	724(?)	726	724 <sup>B</sup> (3)	724		?	
					813		731 <sup>B</sup>		728	ρ(CH <sub>2</sub> )
									753	
			753				778 <sup>sh</sup>			
			756 <sup>sh</sup>		770				788	ω <sub>11</sub>
797 (4)		806	805				787		788	ρ(CH <sub>2</sub> )
							800		799	
					837 <sup>sh</sup>		810		807	
832 <sup>B</sup> (5)			836		844	833 <sup>B</sup> (2)	831		835	γ
									843	
848 <sup>B</sup> (6)						850 <sup>B</sup> (2)	853			

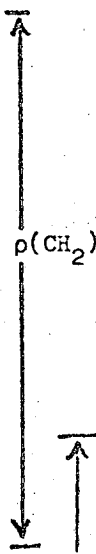


Table II (cont.)

	PAA		PAΦ		PAB		HAB		Assignment (Ref. 6)	
	Ref. 8	Ref. 9	Ref. 6	This work	Ref. 6	This work	Ref. 6	This work		
This work				This work		This work		This work		
911(20)	914		908	911 <sup>B</sup> (8)	914	910(7)	910	910(11)	910	ρ(CH <sub>3</sub> )? ω <sub>1</sub> ω <sub>c</sub>
			943		922		942		935	} γ
			959		938		948		?	
					966		958			
							978			
			1006		1008			988		
							1007 <sup>sh</sup>	1008		δ <sub>5</sub>
		1013								} ω <sub>c-o</sub>
			1020				1017			
		1028						1028		
					1045			1058		
							1060	1068		
		1078								
							1088 <sup>sh</sup>			
1095(36)	1094	1103	1091	1095(27)	1099	1095(17)	1097	1095(31)	1096	
			1109 <sup>sh</sup>		1110 <sup>sh</sup>				1111	} ?δ <sub>4</sub>
114	1112	1122	1115	1114 <sup>B</sup> (11)	1122	1115 <sup>B</sup> (1)	1118	1113 <sup>B</sup> (2)	1118	
		1143		1140 <sup>B</sup> (7)		1142 <sup>B</sup> (14)	1129	1141(100)	1129	τ(CH <sub>2</sub> )



Table II (cont.)

PAA			PAΦ		PAB		HAB		Assignment	
This work	Ref. 8	Ref. 9	Ref. 6	This work	Ref. 6	This work	Ref. 6	This work	Ref. 6	(Ref. 6)
1157 <sup>sh</sup> (6)			1154	1159 <sup>B</sup> (4)	1160	1159 <sup>B</sup> (2)	1157	1156 <sup>B</sup> (3)	1157	$\delta_3$
		1165	1167							
1171(48)	1174	1180	1181	1178(18)	1174 <sup>sh</sup>	1178(18)	1171 <sup>sh</sup>	1176(25)	?	$\gamma(\text{CH}_3)?$ $\tau(\text{CH}_2)$
1186 <sup>sh</sup> (4)		1195				1188(2)		1192(25)	1203 <sup>sh</sup>	
		1203								
1220 <sup>sh</sup> (11)		1225	1218 <sup>sh</sup>	1220(4)	1217	1221(4)	1216 <sup>sh</sup>	1219 <sup>B</sup> (?)	1221 <sup>sh</sup> ?	
1246(85)	1247	1253	1250	1246(32)		1253 <sup>B</sup>		1246(47)	1251 <sup>B</sup>	$\omega_4$
1252(19)			1260	1253(7?)	1258 <sup>B</sup>			1261(19?)		
1261(67)				1262(8?)		* <sup>sh</sup> 1260(28)		1268(75)		
				1271(14)						
1276(100)	1276	1284	1277 <sup>sh</sup>	1280(82)	1278	1271(100)	1270 <sup>sh</sup>	1278(50)	1281	$\omega_3$ $\gamma(\text{CH}_2)$
						1281(11)				
1301 <sup>sh</sup> (5)		1308	1300	1300(?)	1300	1300(?)	1302	1300 <sup>B</sup> (12)	1296 <sup>sh</sup> 1303	
1319 <sup>B,sh</sup> (50)		1328	1311	1319 <sup>sh</sup> (28)	1320	1320 <sup>B,sh</sup> (28)	1320	1320 <sup>B</sup> (41)	1318	$\omega_9, \delta_1?$
1333(87)	1334	1342	1331	1332(100)	1332	1332(44)	1336	1333(47)	1336	$\omega(\text{N.N.o})$
								1367 <sup>sh</sup>	1348 <sup>sh</sup>	
			1370					1380	1382 <sup>sh</sup>	
					1393			1394	1397	
1410(42)	1408	1418	1414	1411(33)	1414	1411(26)	1417	1410(93)	1417	$\omega_9$ or $\delta_1?$
			1425 <sup>sh</sup>		1422 <sup>sh</sup>		1427 <sup>sh</sup>		1425 <sup>sh</sup>	$\delta(\text{CH}_3)$
1438 <sup>B</sup> (4)		1446	1446	1439 <sup>B</sup> (4)	1449 <sup>sh</sup>		1440 <sup>sh</sup>		1438 <sup>sh</sup>	$\omega_5$
1454(36)		1461	1456	1454 <sup>B,sh</sup> (6)	1457 <sup>sh</sup>	1454(40)		1454(50)		$\omega(\text{N.N.o})$ $\delta(\text{CH}_2)$
1465 <sup>*B,sh</sup> (37)	1460	1466	1464	1464(73)	1463	1466 <sup>sh</sup> (2)	1464	1466(65)	1462 <sup>sh</sup>	
		1477	1473					1472 <sup>sh</sup>	1470	
					1477			1481 <sup>sh</sup>		
1501 <sup>B</sup> (18)	1496	1501	1500	1499(18)	1502	1500(8)	1503	1500(22)	1502	$\omega_6$
					1547			1540 <sup>sh</sup>		
1570 <sup>B</sup> (28)	1572		1567	1570(5)	1564			1566	1564	
1582 <sup>sh</sup> (3)				1580 <sup>B</sup> (4)					1580 <sup>B</sup> (10)	
1596(97)				1595(47)		1595 <sup>sh</sup> (7)	1595	1595 <sup>sh</sup> (6)	1594	
1604 <sup>sh</sup> (11)	1603	1605	1600	1604 <sup>B,sh</sup> (19)	1603	1604(21)	1603	1605(69)	1607 <sup>sh</sup>	$\omega_7, \omega_8$
								1626 <sup>sh</sup>	1629 <sup>sh</sup>	
			1648 <sup>sh</sup>		1650 <sup>sh</sup>		1640 <sup>sh</sup>			

† = the accuracy of our frequency determination is  $\pm 2 \text{ cm}^{-1}$ .

\* = Normalized intensity given between parentheses

B = Broad line

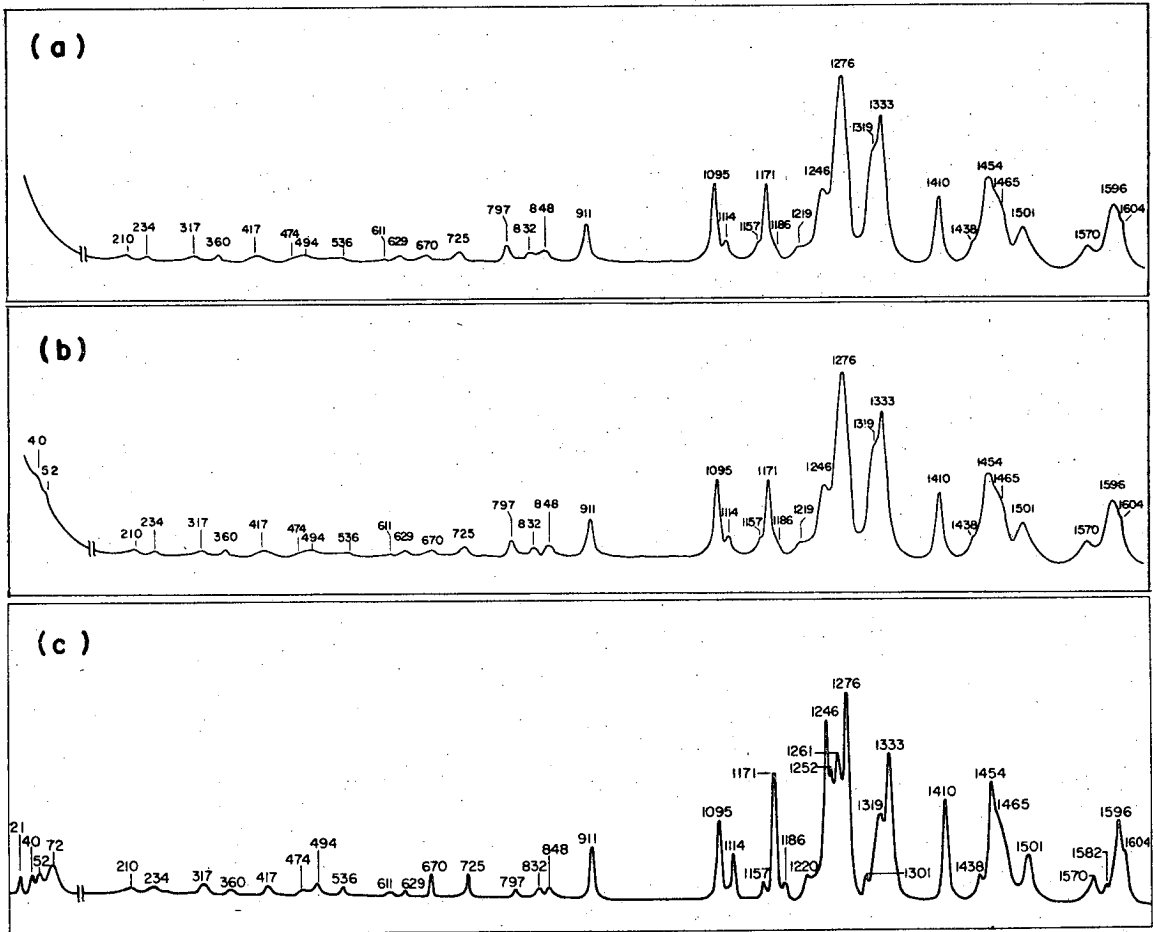
sh = shoulder

## FIGURE CAPTIONS

- Fig. 1. Complete Raman spectra of PAA in the three phases: (a) liquid phase at  $T = 136.7^{\circ}\text{C}$ ; (b) nematic phase at  $T = 116.8^{\circ}\text{C}$ ; (c) solid phase at  $T = 113.9^{\circ}\text{C}$ .
- Fig. 2. Complete Raman spectra of  $\text{PA}\Phi$  in the three phases: (a) liquid phase at  $T = 170.2^{\circ}\text{C}$ ; (b) nematic phase at  $T = 136.9^{\circ}\text{C}$ ; (c) solid phase at  $T = 134.2^{\circ}\text{C}$ .
- Fig. 3. Complete Raman spectra of PAB in the three phases (a) liquid phase at  $T = 125.1^{\circ}\text{C}$ ; (b) nematic phase at  $T = 79.1^{\circ}\text{C}$ ; (c) solid phase at  $T = 76.6^{\circ}\text{C}$ .
- Fig. 4. Complete Raman spectra of HAB in the three phases: (a) liquid phase at  $T = 129.3^{\circ}\text{C}$ ; (b) nematic phase at  $T = 86.1^{\circ}\text{C}$ ; (c) solid phase at  $T = 82.1^{\circ}\text{C}$ .
- Fig. 5. Detailed Raman spectra of PAA in the spectral region of  $1225\text{-}1300\text{ cm}^{-1}$ : (a) solid phase at  $113.9^{\circ}\text{C}$ ; (b) nematic phase at  $116.8^{\circ}\text{C}$ ; (c) liquid phase at  $134.8^{\circ}\text{C}$ .
- Fig. 6. Detailed Raman spectra of  $\text{PA}\Phi$  in the spectral region of  $1225\text{-}1300\text{ cm}^{-1}$ : (a) solid phase at  $134.2^{\circ}\text{C}$ ; (b) nematic phase at  $136.9^{\circ}\text{C}$ ; (c) liquid phase at  $170.2^{\circ}\text{C}$ .
- Fig. 7. Detailed Raman spectra of PAB in the spectral region of  $1225\text{-}1300\text{ cm}^{-1}$ : (a) solid phase at  $76.6^{\circ}\text{C}$ ; (b) nematic phase at  $79.1^{\circ}\text{C}$ ; (c) liquid phase at  $125.1^{\circ}\text{C}$ .
- Fig. 8. Detailed Raman spectra of HAB in the spectral region of  $1225\text{-}1300\text{ cm}^{-1}$ : (a) solid phase at  $82.1^{\circ}\text{C}$ ; (b) nematic phase at  $86.1^{\circ}\text{C}$ ; (c) liquid phase at  $129.3^{\circ}\text{C}$ .

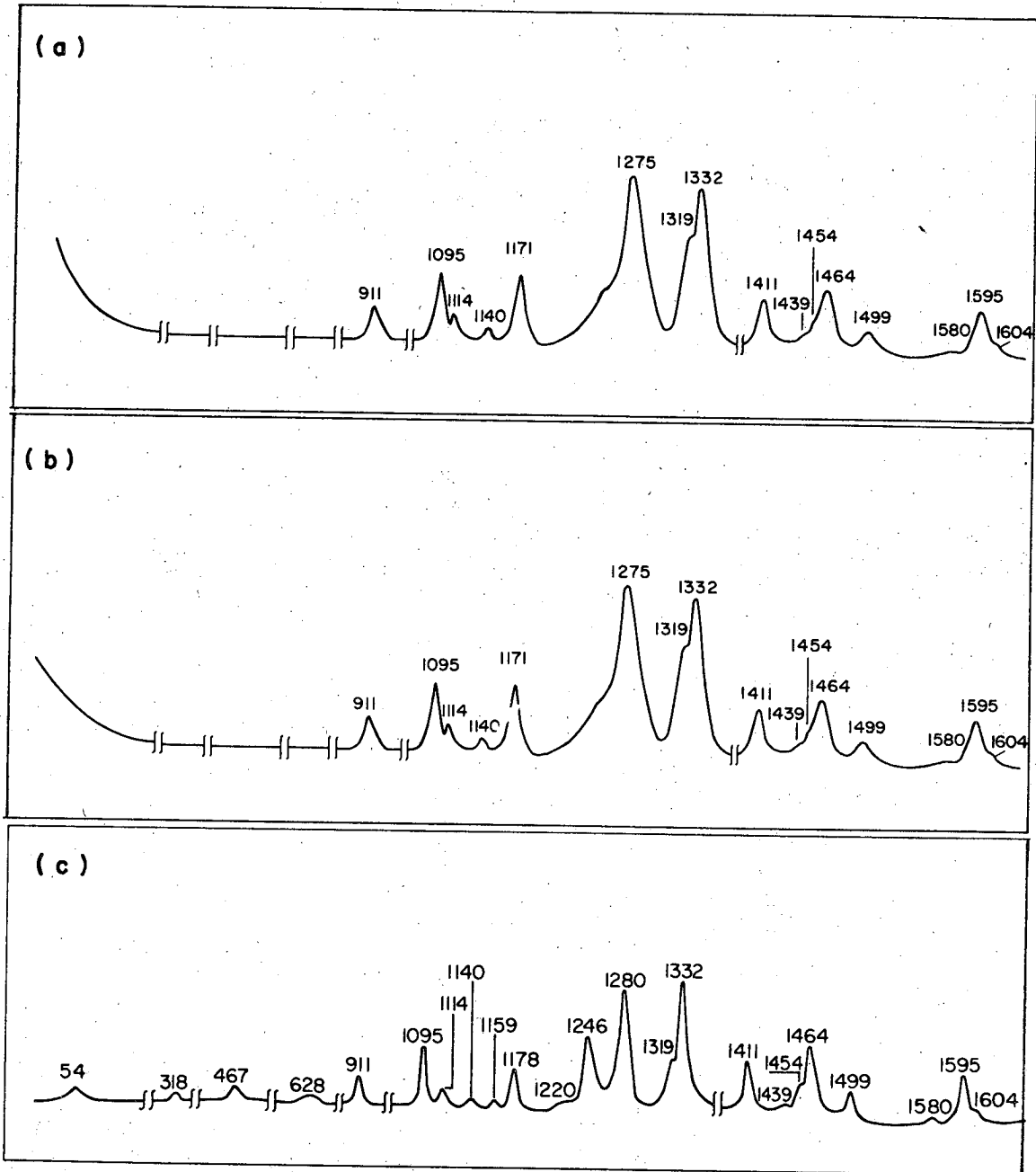
Fig. 9. Normalized integrated intensity of the  $1141 \text{ cm}^{-1}$  mode of HAB as a function of temperature.

Fig. 10. Temperature dependence of the  $1178 \text{ cm}^{-1}$  shift in PAΦ.



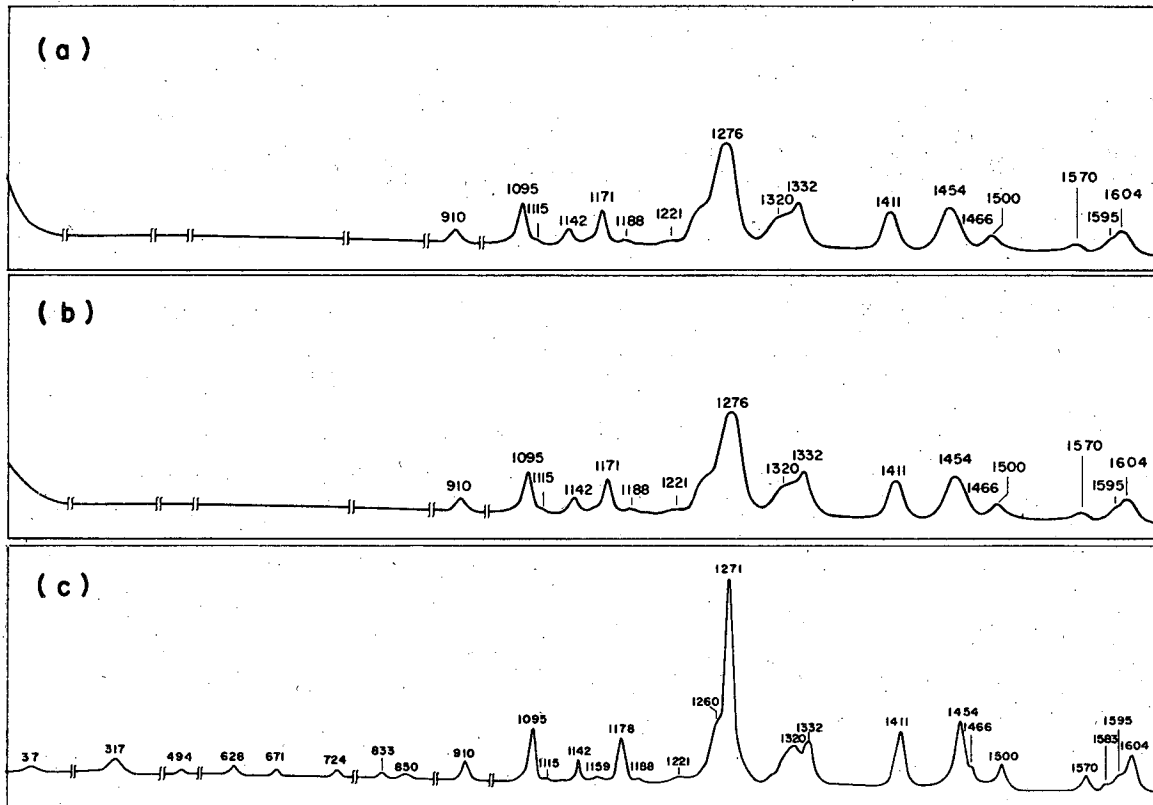
XBL714-3334

Fig. 1



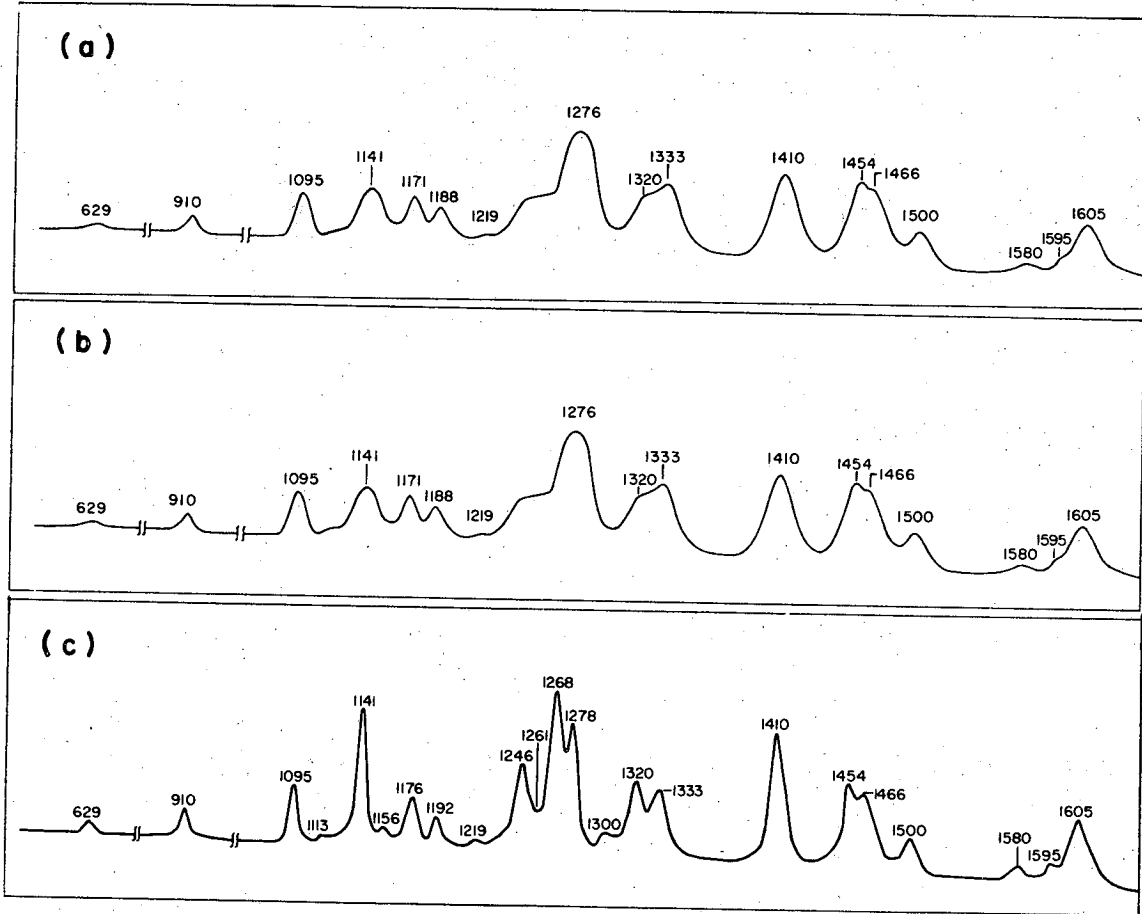
XBL7011-4134

Fig. 2



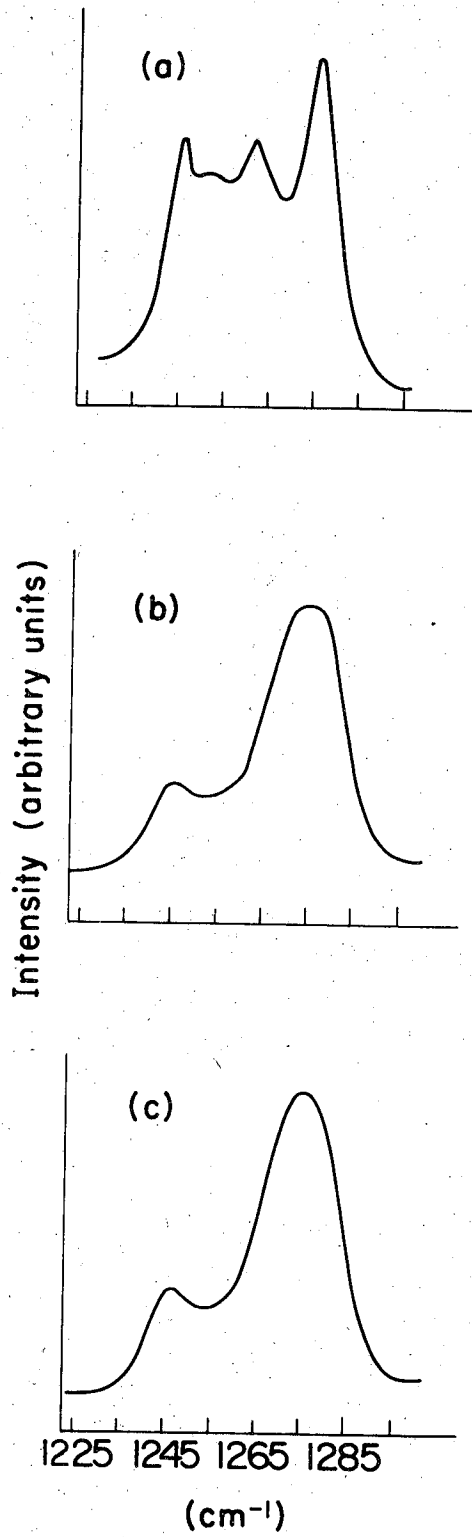
XBL714-3336

Fig. 3



XBL714-3335

Fig. 4



XBL7011-4145

Fig. 5

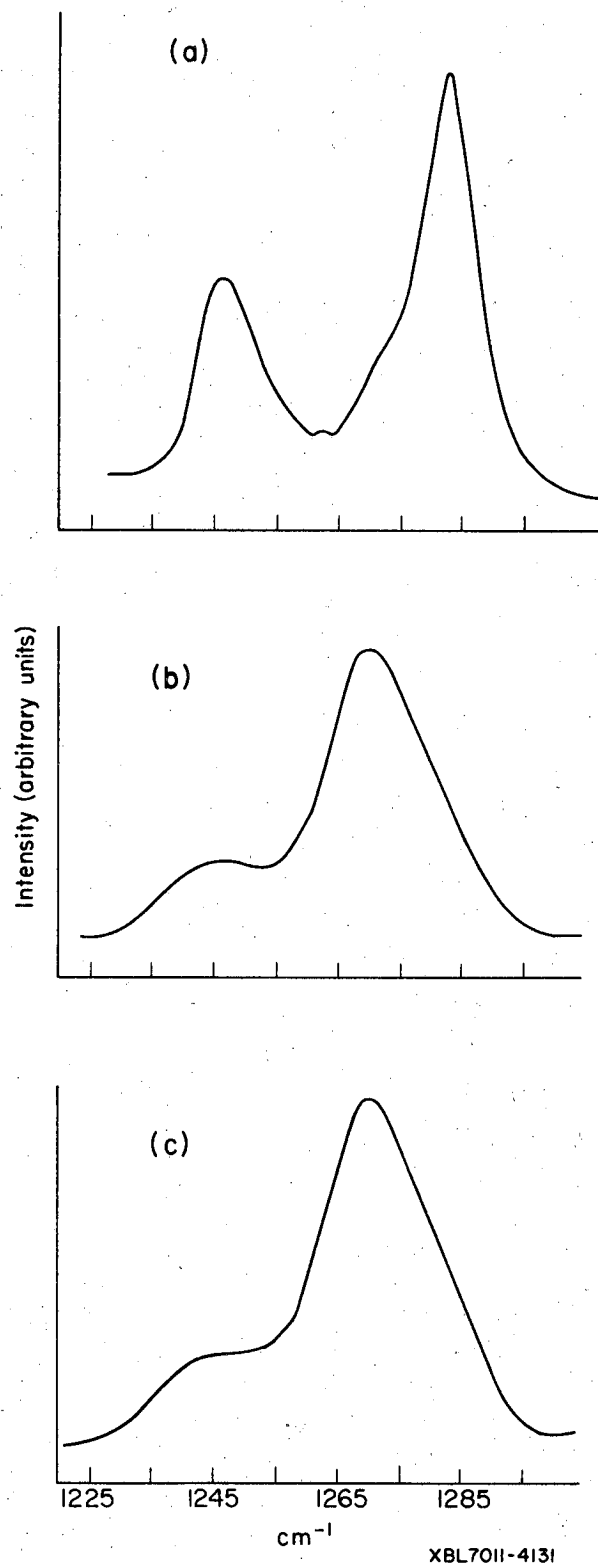


Fig. 6

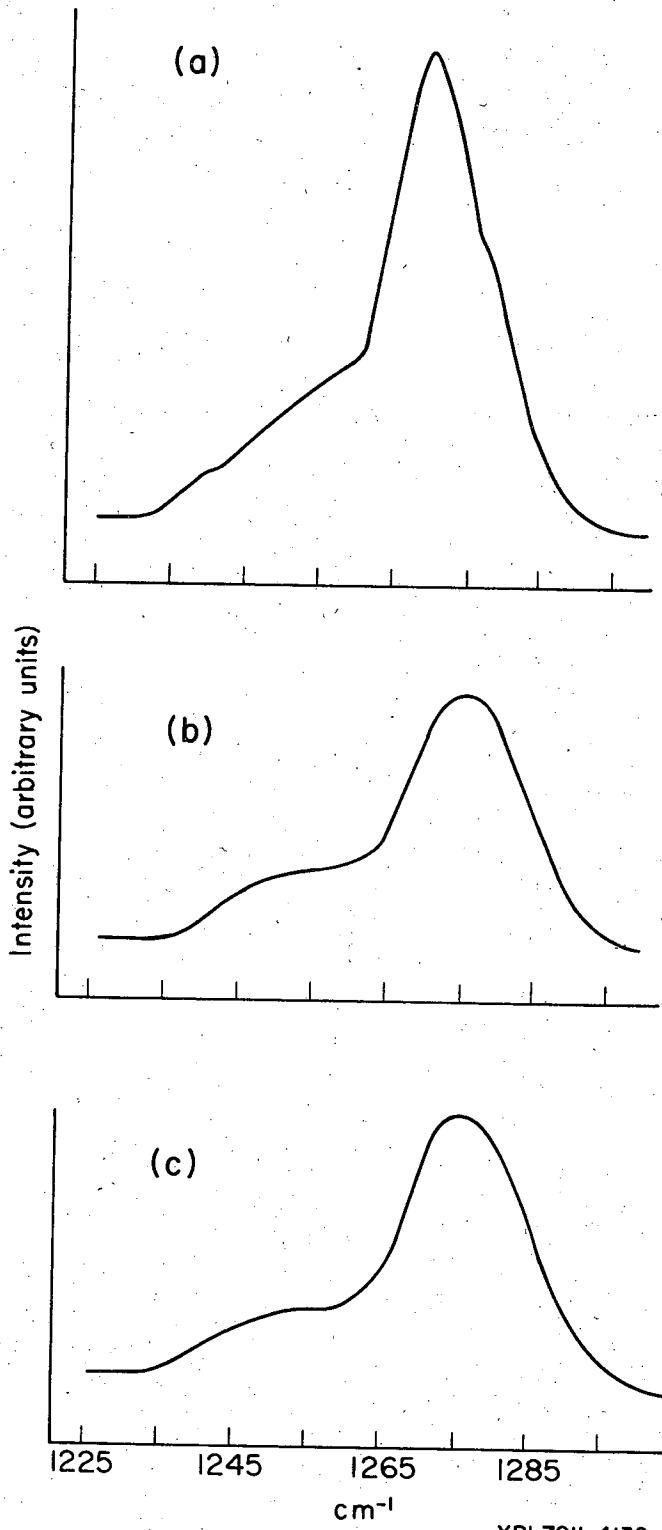
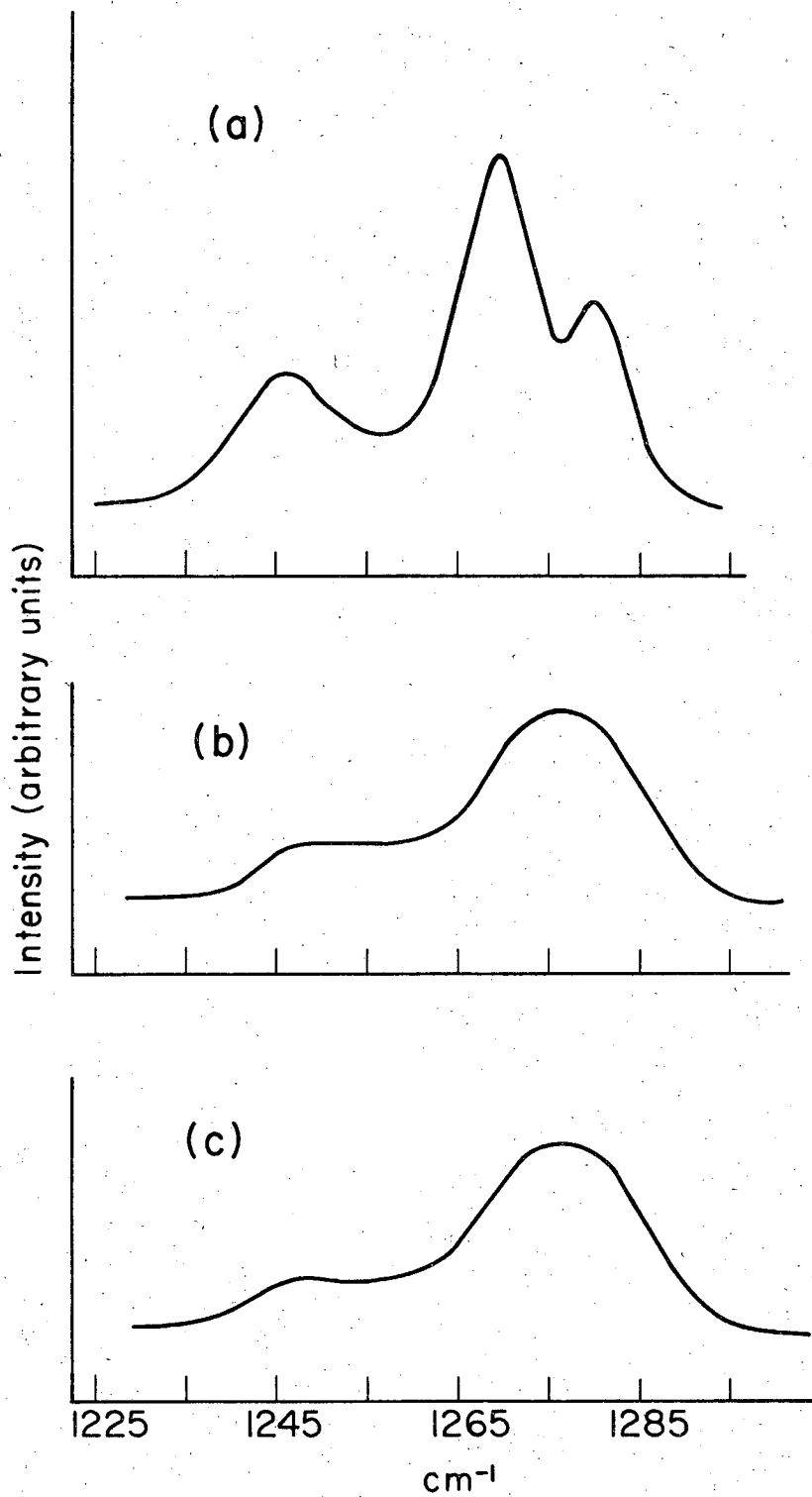
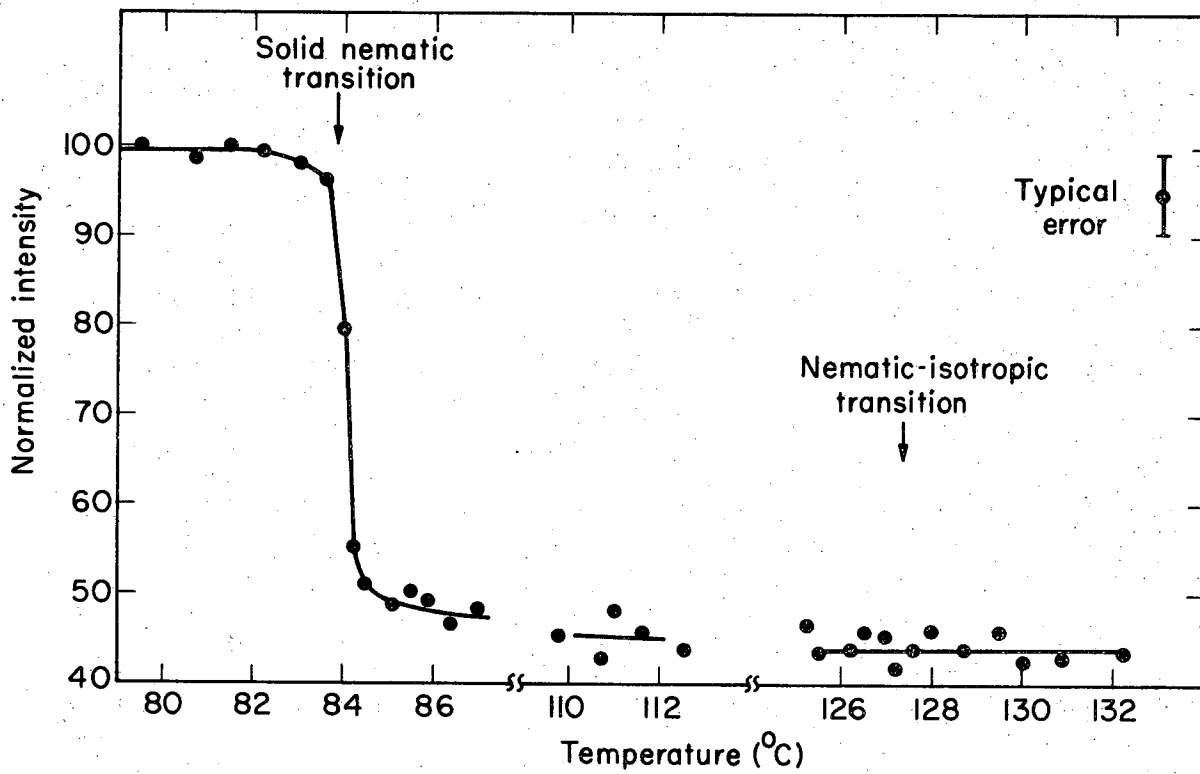


Fig. 7



XBL7011-4128

Fig. 8



XBL7011-4130

Fig. 9

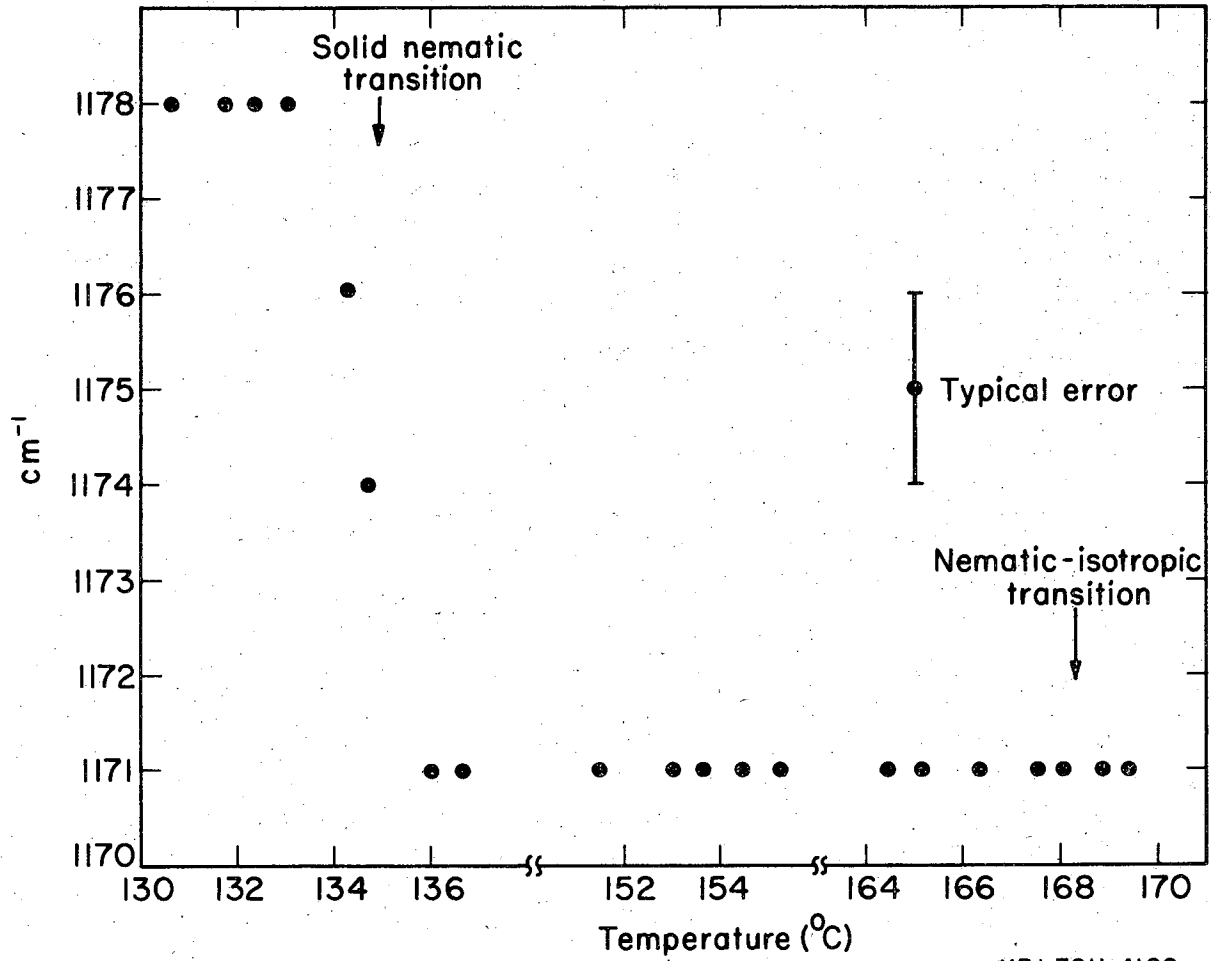


Fig. 10

